*Inorg. Chem.* **2006**, *45*, 1498–1507


# Solution and Structural Investigations of Ligand Preorganization in Trivalent Lanthanide Complexes of Bicyclic Malonamides

**Bevin W. Parks, Robert D. Gilbertson,‡ and James E. Hutchison***

*Chemistry Department, University of Oregon, Eugene, Oregon 97403-1253*

**Elisabeth Rather Healey and Timothy J. R. Weakley**

*X-Ray Crystallography Laboratory, Chemistry Department, University of Oregon, Eugene, Oregon 97403-1253*

**Brian M. Rapko, Benjamin P. Hay, and Sergei I. Sinkov**

*Pacific Northwest National Laboratory, Richland, Washington 99352*

**Grant A. Broker and Robin D. Rogers**

*Center for Green Manufacturing and Department of Chemistry, The University of Alabama, Tuscaloosa, Alabama 35487*

Received March 23, 2005

This report describes an investigation into the coordination chemistry of trivalent lanthanides in solution and the solid state with acyclic and preorganized bicyclic malonamide ligands. Two experimental investigations were performed: solution binding affinities were determined through single-phase spectrophotometric titrations and the extent of conformational change upon binding was investigated with single-crystal X-ray crystallography. Both experimental methods compare the bicyclic malonamide (BMA), which is designed to be preorganized for binding trivalent lanthanides, to an analogous acyclic malonamide. Results from the spectrophotometric titrations indicate that BMA exhibits a 10–100× increase in binding affinity to Ln(III) over acyclic malonamide. In addition, BMA forms compounds with high ligand–metal ratios, even when competing with water and nitrate ligands for binding sites. The crystal structures exhibit no significant differences in the nature of the binding between Ln(III) and the BMA or acyclic malonamide. These results support the conclusion that rational ligand design can lead to compounds that enhance the binding affinities within a ligand class.

## Introduction

The rational design of ligands is a continuing challenge in the design of functional metal complexes for materials, sensors, probes, and medicinal uses and in the field of supramolecular chemistry.[1−5] Ligand design involves the examination of existing metal−ligand complex structures in order to generate computer models. These models aid in the selection and geometric arrangement of donor atoms in order to obtain the desired properties of both the ligand and the resulting metal−ligand complex. Experimental investigation of these designed targets, when correlated with initial design strategies, advances the understanding of structure−function relationships of the metal−ligand complexes. The results of solution and crystallographic studies can be used to refine

* To whom correspondence should be addressed. E-mail: hutch@uoregon.edu.
‡ Present address: Los Alamos National Laboratory, Los Alamos, NM 87545.

(1) Reger, D. L.; Watson, R. P.; Gardinier, J. R.; Smith, M. D. *Inorg. Chem.* **2004**, *43*, 6609−6619.
(2) Dutasta, J.-P. *Top. Curr. Chem.* **2004**, *232*, 55−91.
(3) Braga, D.; Polito, M.; D'Addario, D.; Tagliavini, E.; Proserpio, D. M.; Grepioni, F.; Steed, J. W. *Organometallics* **2003**, *22*, 4532−4538.
(4) Kim, H. K.; Roh, S. G.; Hong, K.-S.; Ka, J.-W.; Baek, N. S.; Oh, J. B.; Nah, M. K.; Cha, Y. H.; Ko, J. *Macromol. Res.* **2003**, *11*, 133−145.
(5) Patra, G. K.; Goldberg, I. *Cryst. Growth Des.* **2003**, *3*, 321−329.



10.1021/ic050437d CCC: $33.50 
Published on Web 01/24/2006

design models, further increasing the chances of obtaining enhanced properties in subsequently developed targets. Each iteration affords a greater understanding of ligand−metal interactions and accelerates the transition into de novo ligand design.

We have applied the principles of rational ligand design to the malonamide ligand−trivalent lanthanide system. Malonamide ligands have been studied as extractants of trivalent lanthanides from nuclear waste for the diamide extraction (DIAMEX) process, a remediation process under development.[6−17] Malonamides are selective toward trivalent lanthanides[18] and are unusual because they are a neutral ligand that can successfully compete with coordinated water for a binding site on a lanthanide ion in an aqueous environment.[19] Extensive research concerning the complexation of malonamides with trivalent lanthanides[7,9,18,20−24] has led to modest improvements in the extraction efficiencies.[18,22,24] One factor that limits the effectiveness of acyclic malonamides as extractants is the strain induced in the ligand upon complexation to the metal.[25] Knowledge of the limitations imposed by ligand strain provides an opportunity for improvement through rational design.

Previous investigations of the acyclic malonamide/Ln(III) system revealed that the amide carbonyls align away from one another in order to balance the dipole moment; this causes the free ligand to be in an unfavorable conformation in comparison to the conformation of the ligand bound to a metal.[25−28] For the least sterically hindered malonamide structure, tetramethylmalonamide (TMMA), molecular mechanics calculations predict that an overall strain energy of 5.5 kcal/mol is induced upon chelation of a trivalent lanthanide.[25]

**Chart 1.** Acyclic Malonamide Ligands and Preorganized Bicyclic Malonamide Ligands

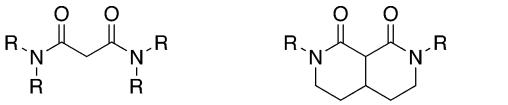


To overcome the considerable strain generated in an acyclic malonamide upon binding, we focused upon the development of a conformationally preorganized malonamide ligand in which the most populated conformation of the free ligand approaches that of the bound conformation of the ligand. Such preorganized ligands should experience minimal strain upon binding, which should translate into an increased binding affinity. Each ligand under consideration was fitted to a model lanthanide ion (Eu(III)) and optimized using molecular mechanics calculations. From this evaluation, the fused 6,6-bicyclic malonamide (BMA) was chosen as the target preorganized ligand because the lowest-energy conformation of the free ligand and the optimal ligand conformation for binding Ln(III) were structurally similar, indicating a high degree of preorganization.[25,29,30]

Preorganized ligands with methyl and octyl substituents, $Me_2$BMA and $Oct_2$BMA (see Chart 1), were synthesized and studied for an initial assessment of the success of the design process.[25] X-ray crystallography of a Eu(III) complex with $Me_2$BMA shows that the bound ligand matches the ligand structure predicted by the molecular mechanics calculations.[25] Extraction studies of Eu(III) comparing $Oct_2$BMA and a model acyclic malonamide, tetrahexylmalonamide (THMA), showed a $10^7$-fold increase in extraction efficiency with the conformationally limited bicyclic ring structure.[25,30] Single-phase binding affinity studies of $Me_2$BMA and TMMA with multivalent actinide ions [U(VI), Np(V), Pu(IV/VI), Am(III)] also showed greatly enhanced binding of the preorganized $Me_2$BMA over TMMA.[31,32] These results indicate that the rational approach to preparing a more effective complexant for binding to f-block metals was successful.

(6) Berthon, L.; Morel, J. M.; Zorz, N.; Nicol, C.; Virelizier, H.; Madic, C. *Sep. Sci. Technol.* **2001**, *36*, 709−728.
(7) Courson, O.; Lebrun, M.; Malmbeck, R.; Pagliosa, G.; Romer, K.; Satmark, B.; Glatz, J. P. *Radiochim. Acta* **2000**, *88*, 857−863.
(8) Erlinger, C.; Gazeau, D.; Zemb, T.; Madic, C.; Lefrancois, L.; Hebrant, M.; Tondre, C. *Solvent Extr. Ion Exch.* **1998**, *16*, 707−738.
(9) Facchini, A.; Amato, L.; Modolo, G.; Nannicini, R.; Madic, C.; Baron, P. *Sep. Sci. Technol.* **2000**, *35*, 1055−1068.
(10) Grouiller, J.-P.; Pillon, S.; de Saint Jean, C.; Varaine, F.; Leyval, L.; Vambenepe, G.; Carlier, B. *J. Nucl. Mater.* **2003**, *320*, 163−169.
(11) Kumbhare, L. B.; Prabhu, D. R.; Mahajan, G. R.; Sriram, S.; Manchanda, V. K.; Badheka, L. P. *Nucl. Technol.* **2002**, *139*, 253−262.
(12) Madic, C.; Bourges, J.; Dozol, J.-F. *AIP Conf. Proc.* **1995**, *346*, 628−638.
(13) Madic, C.; Hudson, M. J.; Liljenzin, J.-O.; Glatz, J.-P.; Nannicini, R.; Facchini, A.; Kolarik, Z.; Odoj, R. *Prog. Nucl. Energy* **2002**, *40*, 523−526.
(14) Malmbeck, R.; Courson, O.; Pagliosa, G.; Romer, K.; Satmark, B.; Glatz, J. P.; Baron, P. *Radiochim. Acta* **2000**, *88*, 865−871.
(15) Manchanda, V. K.; Pathak, P. N.; Rao, A. K. *Solvent Extr. Ion Exch.* **2004**, *22*, 353−375.
(16) Modolo, G.; Seekamp, S.; Nabett, S. *Chem.-Ing.-Technol.* **2002**, *74*, 261−265.
(17) Sood, D. D.; Patil, S. K. *J. Radioanal. Nucl. Chem.* **1996**, *203*, 547−573.
(18) Spjuth, L.; Liljenzin, J. O.; Skalberg, M.; Hudson, M. J.; Chan, G. Y. S.; Drew, M. G. B.; Feaviour, M.; Iveson, P. B.; Madic, C. *Radiochim. Acta* **1997**, *78*, 39.
(19) Aspinall, H. C. *Chemistry of the f-Block Elements*; Overseas Publishers Association: Amsterdam, 2001; Vol. 5.
(20) Chan, G. Y.; Drew, M. G. B.; Hudson, M. J.; Iveson, P. B.; Liljenzin, J. O.; Skalberg, M.; Spjuth, L.; Madic, C. *J. Chem. Soc., Dalton Trans.* **1997**, 649.
(21) Tan, X.-F.; Wang, Y.-S.; Tan, T.-Z.; Zhou, G.-F.; Bao, B.-R. *J. Radioanal. Nucl. Chem.* **1999**, *242*, 123.
(22) McNamara, B. K.; Lumetta, G. J.; Rapko, B. M. *Solvent Extr. Ion Exch.* **1999**, *17*, 1403.
(23) Lumetta, G. J.; McNamara, B. K.; Rapko, B. M.; Hutchison, J. E. *Inorg. Chim. Acta* **1999**, *293*, 195.
(24) Spjuth, L.; Liljenzin, J. O.; Hudson, M. J.; Drew, M. G. B.; Iveson, P. B.; Madic, C. *Solvent Extr. Ion Exch.* **2000**, *18*, 1.
(25) Lumetta, G. J.; Rapko, B. M.; Garza, P. A.; Hay, B. P.; Gilbertson, R. D.; Weakley, T. J. R.; Hutchison, J. E. *J. Am. Chem. Soc.* **2002**, *124*, 5644−5645.
(26) Sandrone, G.; Dixon, D. A.; Hay, B. P. *J. Phys. Chem. A* **1999**, *103*, 3554.
(27) Hay, B. P.; Clement, O.; Sandrone, G.; Dixon, D. A. *Inorg. Chem.* **1998**, *37*, 5887.
(28) Clement, O.; Rapko, B. M.; Hay, B. P. *Coord. Chem. Rev.* **1998**, *170*, 203.
(29) Hay, B. P.; Firman, T. K.; Lumetta, G. J.; Rapko, B. M.; Garza, P. A.; Sinkov, S. I.; Hutchison, J. E.; Parks, B. W.; Gilbertson, R. D.; Weakley, T. J. R. *J. Alloys Compd.* **2004**, *374*, 416−419.
(30) Lumetta, G. J.; Rapko, B. M.; Hay, B. P.; Garza, P. A.; Hutchison, J. E.; Gilbertson, R. D. *Solvent Extr. Ion Exch.* **2003**, *21*, 29−39.
(31) Sinkov, S. I.; Rapko, B. M.; Lumetta, G. J.; Hutchison, J. E.; Parks, B. W. *AIP Conf. Proc.* **2003**, *673*, 36−38.
(32) Sinkov, S. I.; Rapko, B. M.; Lumetta, G. J.; Hay, B. P.; Hutchison, J. E.; Parks, B. W. *Inorg. Chem.* **2004**, *43*, 8404−8413.

Since the original calculations were based upon a trivalent lanthanide, it was of interest to perform an in-depth study with this group. A series of the chemically similar trivalent lanthanides is a simple, large group of metal ions changing only in ionic radius, and so provides a good basis set for a comparison of $Me_2BMA$ and TMMA. Analysis of a series also indicates whether the previously observed improvements are general to the malonamide−Ln(III) system or if there is a dependence upon the size of the metal ion. The complexity of liquid−liquid extraction makes it very difficult to determine how much of the previously noted lanthanide extraction by the bicyclic ligand is due directly to an increase in binding affinity. By switching to the water-soluble derivatives, a simpler approach involving single-phase spectrophotometric titrations can be used to directly measure the enhancement in binding affinity of $Me_2BMA$ over TMMA. These same derivatives can be used to assess the conformational preorganization via comparison of crystal structures of the free bicyclic malonamide ligand to those of $Me_2BMA$ and TMMA when complexed to trivalent lanthanides. Since the solution and crystallographic studies are performed within the same series of metals (trivalent lanthanides), it is possible to correlate the binding affinities to the observed crystal structures and draw broader conclusions than is possible through either investigation alone.

The combined results of the solution and crystallographic studies reported here suggest that ligand preorganization plays a significant role in the increased binding affinities and the previously reported enhanced extraction efficiencies of the bicyclic malonamides.[25] Spectrophotometric titration studies of a series of trivalent lanthanides show a consistent increase of 1−2 orders of magnitude in binding affinity and a tendency for higher ligand−metal ratios with the bicyclic ligand than with the acyclic ligand. In the solid state, the preorganization indicated by the first Eu−$Me_2BMA$ complex has been confirmed by the study of a series of lanthanide complexes. There is little difference in the conformation of free $Me_2BMA$ and both bound ligands ($Me_2BMA$ and TMMA) in the X-ray crystal structures, confirming conformational preorganization of the ligand $Me_2BMA$ for binding trivalent lanthanides.

## Experimental Section

All experiments were performed under ambient conditions. Methanol was distilled over magnesium turnings under a nitrogen atmosphere. Acetonitrile and ether were purchased from Mallinckrodt and used without purification. Nuclear magnetic resonance (NMR) spectra were gathered on a Varian Unity INOVA 300 MHz spectrometer (299.95 MHz). Ultraviolet−visible (UV−vis) measurements were made on a 400-series charge-coupled device (CCD) array spectrophotometer (Spectral Instruments, Inc.) with a 200−950 nm spectral range. The solutions were held in PLASTIBRAND 1 cm cuvettes with an optical transparency range of 220−900 nm. Lanthanide nitrate salts were purchased in hydrate form from Aldrich and used as supplied. TMMA was purchased from TCI and used without purification. $Me_2BMA$ was synthesized as previously reported and characterized by $^1H$ and $^{13}C$ NMR and UV−vis spectroscopy.[25]

**Preparation of Metal Complexes for Single-Crystal X-Ray Structure Determination.** In each case, the metal salt (0.2 mmol) was dissolved in methanol (5 mL) and a solution of the ligand (0.6 mmol) in methanol (2 mL) was added dropwise to the well-stirred metal solution. The solution was heated to gentle reflux (30 min) then allowed to evaporate to a viscous oil under a stream of dry $N_2$. $Et_2O$ (10 mL) was added, and the solution was triturated vigorously for 5 min. The $Et_2O$ was decanted off, and the sample was triturated with a fresh 10 mL $Et_2O$ for 5 min. This trituration procedure was repeated until an off-white powder was obtained (typically three times) then repeated an additional two times with the powder material. The residual solid was placed under vacuum overnight to remove the remaining $Et_2O$. In a 2 dram vial, about 40 mg of the dried solid was dissolved in 0.5 mL of acetonitrile and crystallized using a vapor diffusion method with diethyl ether as the poor solvent.

**X-Ray Crystallography Data Collection.** Table 1 reports details of the structural analyses for all of the complexes. X-ray crystallography data collection was carried out using a Siemens SMART diffractometer with a CCD area detector, using graphite-monochromated Mo Kα radiation. The SHELXTL software, version 5, was used for solutions and refinement.[33] Absorption corrections were made with SADABS.[34] The structures were refined by full-matrix least-squares on $F^2$. All nonhydrogen atoms were anisotropically refined, while all hydrogen atoms were included in calculated positions and refined using a riding model. None of the structures exhibited any unusual features in the solution or refinement process.

**Spectrophotometric Titrations.** Aqueous metal working solutions were produced from their respective metal salts. The solution concentrations were determined by visible spectroscopy using the molar absorptivity of a strong reference peak ($\lambda_{ref}$). The titrations were monitored by the change in molar absorptivity of the hypersensitive band ($\lambda_{hyp}$), a 4f → 4f transition that is very sensitive to the ligand environment. Metal salts and peaks with the corresponding molar absorptivity are as follows: Nd(III); $Nd(ClO_4)_3$; $\lambda_{ref}$ = 576 nm ($\epsilon$ = 7.20 $cm^{-1}$ $M^{-1}$); $\lambda_{hyp}$ = 576 nm ($\epsilon$ = 7.20 $cm^{-1}$ $M^{-1}$). Eu(III); $Eu(OSO_2CF_3)_3$; $\lambda_{ref}$ = 393 nm ($\epsilon$ = 2.77 $cm^{-1}$ $M^{-1}$); $\lambda_{hyp}$ = 465 nm ($\epsilon$ = 0.05 $cm^{-1}$ $M^{-1}$). Ho(III); $Ho(NO_3)_3$; $\lambda_{ref}$ = 451 nm ($\epsilon$ = 3.90 $cm^{-1}$ $M^{-1}$); $\lambda_{hyp}$ = 451 nm ($\epsilon$ = 3.90 $cm^{-1}$ $M^{-1}$). Er(III); $Er(ClO_4)_3$; $\lambda_{ref}$ = 523 nm ($\epsilon$ = 3.40 $cm^{-1}$ $M^{-1}$); $\lambda_{hyp}$ = 523 ($\epsilon$ = 3.40 $cm^{-1}$ $M^{-1}$) and 379 nm ($\epsilon$ = 6.68 $cm^{-1}$ $M^{-1}$).[35]

Spectrophotometric titrations were performed by first introducing a portion of the starting metal solution directly into the cuvette. The ligand then was introduced either by dissolution of aliquots of neat TMMA or preweighed solid portions of $Me_2BMA$ directly into the cuvette. The increase in solution volume after each step of ligand addition and dissolution was estimated on the basis of a calibration plot obtained in separate experiments for each ligand. All solution spectra were referenced to a blank solution containing the supporting electrolyte (1.0 M $HNO_3$).

All spectra were taken over the widest range possible. Reliable data could not be obtained below 330 nm because the nitrate ion strongly absorbs below this region and the cuvette limited the upper range to 900 nm. The data processing ranges were selected around the hypersensitive peaks of lanthanide cations as follows: Nd(III),

(33) Sheldrick, G. M. *SHELXTL*, 5.05 ed.; Siemens Analytical X-ray Instruments: Madison, WI, 1996.
(34) Sheldrick, G. M. *Program for Semiempirical Absorption Correlation of Area Detector Data*; University of Göttingen: Göttingen, Germany, 1996.
(35) Carnall, W. T. In *Handbook on the Physics and Chemistry of Rare Earths*; Gschneidner, K. A., Jr., Eyring, L., Eds.; North-Holland: New York, 1979; pp 171−208.

**Table 1.** Crystallographic Data and Refinement Details for the Reported Complexes

| | $Me_2BMA$ | $La-Me_2BMA$ | $Nd-Me_2BMA$ | $Eu-Me_2BMA$ | $Gd-Me_2BMA$ |
|---|---|---|---|---|---|
| formula | $C_{10}H_{16}N_2O_2$ | $C_{22}H_{36}LaN_8O_{13.5}$ | $C_{20}H_{32}N_7NdO_{13}$ | $C_{20}H_{32}EuN_7O_{13}$ | $C_{20}H_{32}GdN_7O_{13}$ |
| *a* (Å) | 9.356(1) | 10.001(2) | 10.234(2) | 10.243(1) | 10.1554(4) |
| *b* (Å) | 10.222(1) | 11.211(2) | 14.522(2) | 14.424(3) | 14.3680(6) |
| *c* (Å) | 20.934(3) | 15.158(3) | 18.984(2) | 18.920(2) | 18.8152(8) |
| α | 90 | 92.44(3) | 90 | 90 | 90 |
| *β* | 99.68(1) | 105.58(3) | 90 | 90 | 90 |
| *γ* | 90 | 96.81(3) | 90 | 90 | 90 |
| *V* (Å) | 1973.6(5) | 1620.6(2) | 2821.3(5) | 2795.3 | 2745.4(2) |
| *Z* | 8 | 2 | 4 | 4 | 4 |
| fw (g/mol) | 196.25 | 767.5 | 722.75 | 730.47 | 735.78 |
| space group | *C*2/*c* | *P*1 | $P2_12_12_1$ | $P2_12_12_1$ | $P2_12_12_1$ |
| *T* (°C) | 23 | 23 | 23 | 23 | −120 |
| *l* (Å) | 0.71073 | 0.71073 | 0.71073 | 0.71073 | 0.71073 |
| $D_{calc}$ (g/cm) | 1.321 | 1.573 | 1.701 | 1.736 | 1.780 |
| *m* ($cm^{-1}$) | 0.93 | 13.91 | 19.14 | 23.15 | 24.93 |
| *R* ($F_o$) | 0.043 | 0.0352 | 0.044 | 0.027 | 0.0301 |
| $R_w$ ($F_o$) | 0.049 | 0.0953 | 0.048 | 0.03 | 0.0612 |
| | | $La-TMMA$ | $Nd-TMMA$ | $Eu-TMMA$ | $Gd-TMMA$ |
| formula | | $C_{14}H_{28}LaN_7O_{13}$ | $C_{14}H_{28}NdN_7O_{13}$ | $C_{14}H_{28}EuN_7O_{13}$ | $C_{14}H_{28}GdN_7O_{13}$ |
| *a* (Å) | | 10.7904(3) | 10.716(1) | 10.6595(5) | 13.0844(5) |
| *b* (Å) | | 16.4723(4) | 16.3446(2) | 16.2631(8) | 11.3437(4) |
| *c* (Å) | | 14.5036(4) | 14.4342(2) | 14.3906(7) | 15.8016(6) |
| α | | 90 | 90 | 90 | 90 |
| *β* | | 100.350(1) | 100.542(1) | 100.636(1) | 98.189(1) |
| *γ* | | 90 | 90 | 90 | 90 |
| *V* (Å) | | 2536.0(1) | 2485.39(5) | 2451.8(2) | 2321.5(2) |
| *Z* | | 4 | 4 | 4 | 4 |
| fw (g/mol) | | 641.34 | 646.67 | 654.39 | 659.68 |
| space group | | $P2_1/n$ | $P2_1/n$ | $P2_1/n$ | $P2_1/n$ |
| *T* (°C) | | −100 | −100 | −100 | −120 |
| *l* (Å) | | 0.71073 | 0.71073 | 0.71073 | 0.71073 |
| $D_{calc}$ (g/cm) | | 1.680 | 1.728 | 1.773 | 1.887 |
| *m* ($cm^{-1}$) | | 17.57 | 21.63 | 26.33 | 29.36 |
| *R* ($F_o$) | | 0.0304 | 0.0201 | 0.0654 | 0.0258 |
| $R_w$ ($F_o$) | | 0.0535 | 0.0462 | 0.1201 | 0.0537 |

560−600 nm; Eu(III), 461−475 nm; Ho(III), 440−465 nm; and Er(III), 370−387 and 511−535 nm.

**Data Analysis.** Singular value decomposition (SVD) analysis[7] was employed to determine the number of spectrophotometrically distinct species in the optical absorbance spectral data sets collected during spectrophotometric titrations. This method is based on a statistical analysis, free of any chemical model, and does not use any a priori assumptions of chemical nature; the analysis assumes only the validity of the Beer−Lambert law of optical absorbance for multicomponent mixtures.

The number of spectroscopically identifiable species determined by SVD analysis was used to choose a chemical model for the input file of SQUAD (**S**tability **Qu**otients from **A**bsorbance **D**ata—a nonlinear spectra processing routine that considers the series of titration data, the metal-to-ligand ratio from SVD, and the concentrations of metal and ligand in order to calculate the formation constants).[36,37] A modified version of the SQUAD code was employed to refine the stability constants of the light absorbing complexes of the 4f metal cations from the relevant spectral sets.[36,37]

## Results and Discussion

The primary goals of this work were to investigate the extent of conformational preorganization in this bicyclic malonamide in a series of complexes of trivalent lanthanides and to determine the effect of preorganization on the binding affinities with the same lanthanides. The complexes and binding affinities of the bicyclic malonamide, $Me_2BMA$, were compared to those of the analogous acyclic malonamide, TMMA. The solution-phase complexation behavior of $Me_2BMA$ and TMMA with Nd(III), Eu(III), Ho(III), and Er(III) was investigated via single-phase spectrophotometric titrations. The conformational preorganization of $Me_2BMA$ was analyzed by comparison of crystal structures of free $Me_2BMA$ and complexes of $Me_2BMA$ and TMMA with Nd(III), Eu(III), and Gd(III).

**Ligand−Metal Complexes in 1 M Nitric Acid Matrix.** The studies described herein are designed to directly probe the metal-to-ligand ratios and binding affinities for the malonamide ligands with a series of trivalent lanthanides in solutions mimicking extraction conditions. Such data typically are obtained by monitoring formation of the ligand−metal complex during titration via NMR, IR, or UV−vis spectroscopy or by calorimetry. We have found UV−vis spectroscopy to be a convenient method to use with lanthanides because their f−f transitions have sharp, characteristic absorbance peaks in this region.[35] Although most of these transitions are insensitive to changes in the metal's environment, the so-called hypersensitive peaks are good indicators of ligand binding events.[38] Hypersensitive transitions allow direct monitoring of complex formation as the

(36) Leggett, D. J. In *Computational Methods for the Determination of Formation Constants*; Leggett, D. J., Ed.; Plenum Press: New York, 1985; Chapter 6.

(37) Bozhenko, E. I. In *Second International Symposium on Knowledge Acquisition, Representation and Processing (KARP-95)*; Auburn University: Auburn, AL, 1995; pp 10−13.

(38) Misra, S. N.; Sommerer, S. O. *Appl. Spectrosc. Rev.* **1991**, *26*, 151−202.

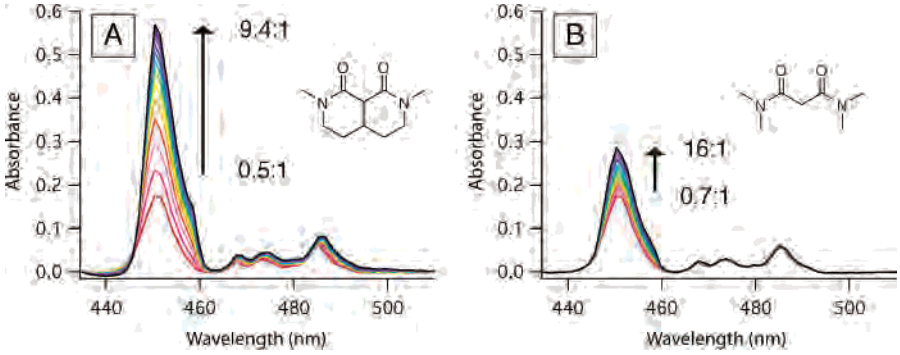


**Figure 1.** UV−vis spectra of Ho(III) spectrophotometric titrations in 1M $HNO_3$ with $Me_2BMA$ (A) and TMMA (B). The bottom spectrum (red line) is the Ho(III) solution before addition of ligand. Arrows indicate change in absorption with increasing ligand-to-metal ratios (values shown to the right of the arrows). The observed increase in intensity in the peak at 451 nm correlates to the ligand binding to the Ho(III) ion.

molar absorptivities of these peaks change strongly when ligands bind.[38] In this study, binding affinities were determined from the changes in absorbance spectra and formation constants for both ligands, $Me_2BMA$ and TMMA, were calculated for a series of trivalent lanthanides. These values were compared directly to determine whether preorganization of the malonamide in the bicyclic ligand results in enhanced binding to trivalent lanthanides.

Spectrophotometric titrations of $Me_2BMA$ and TMMA were attempted with all commercially available lanthanides possessing suitable transitions in the ultraviolet or visible spectrum. To provide viable data, the metal ion must have at least one hypersensitive transition of suitable wavelength and molar absorptivity. The wavelength of the transition must be within the UV−vis detection limits and not overlap with the ligand or nitrate absorptions. The molar absorptivity must be sufficient to accommodate the small initial metal concentrations necessary to achieve the required large excesses of ligand without exceeding the volume of the cuvette. The lanthanide ions discussed in this report [Nd(III), Eu(III), Ho(III), and Er(III)] met these requirements; other lanthanide ions [Pr(III), Sm(III), Dy(III), and Tm(III)] did not.[35]

In each spectrophotometric titration series, a spectrum was collected for the aqueous solution of the metal in 1 M $HNO_3$.[39] Aqueous 1 M $HNO_3$ was selected as the medium for these measurements to allow for direct comparison to the ligands used for extraction in the DIAMEX process and comparison to the previously reported Eu(III) extraction data of $Oct_2BMA$ and THMA.[25] The extraction conditions require a ligand which can bind in 1 M $HNO_3$, so this medium was used despite the competition from water and nitrate ligands. Each addition of ligand is expected to increase the intensity of the hypersensitive peak in proportion to the extent of complex formation.[38] A representative series of spectra for the titration of Ho(III) with $Me_2BMA$ (A) and TMMA (B) is shown in Figure 1. The initial spectrum (bottom red line) is the nitric acid solution of Ho(III) containing no malonamide ligand. The initial Ho(III) concentration was calculated [using the transition at 451 nm ($\epsilon = 3.9$ cm$^{-1}$ M$^{-1}$)] to be 0.0451 M for Figure 1A and 0.0446 M for Figure 1B. The titrations of $Me_2BMA$ and TMMA began with the same metal concentration, and the spectra are displayed on the same scale for ease of comparison. The ligand-to-metal ratios show that less bicyclic ligand is required for more spectral response, a visual display of the enhanced binding of $Me_2BMA$ over TMMA. Of significant note is that the binding affinities of neutral ligands with f-block ions are not normally measurable in aqueous solutions.[19] Competition from water and nitrate make the conditional binding affinities significantly lower than they would be in noncompeting media, as demonstrated by the previously reported log $K_1$ of TMMA to Eu(III) in acetonitrile ($2.48 \pm 0.05$).[40] That malonamide ligands provide any measurable response in the presence of excess water and nitrate ligands further demonstrates their strong affinity for trivalent lanthanides and their potential usefulness in the extraction of trivalent lanthanides from the nuclear waste stream. Sixteen molar equivalents of TMMA is necessary to achieve the same increase in intensity of the Ho(III) hypersensitive absorption achieved with one molar equivalent of $Me_2BMA$. Each of the metal−ligand titrations resulted in a group of spectra similar to that in Figure 1, with a dramatic increase in the hypersensitive peak for the $Me_2BMA$ titration and a smaller increase in the same peak for the TMMA titration.

Changes in the spectrum during the titration of $Me_2BMA$ surprisingly extend to transitions that do not normally exhibit hypersensitivity. In the titration of Ho(III) (see Figure 1), the hypersensitive transition at 451 nm increased in intensity with addition of TMMA and increased to a greater extent with $Me_2BMA$. The transitions from 465 to 490 nm were not expected to change at all and did not with the addition of TMMA. However, the addition of $Me_2BMA$ resulted in increased absorption of those transitions. Changes in peaks that do not meet the selection rules for hypersensitivity have been observed previously in the presence of some ligands and have been termed ligand-mediated pseudohypersensitive transitions (LMPHT).[38] LMPHTs are not observed in any of the TMMA titrations.

To obtain a quantitative value for the increase in binding affinity, the spectral segment including the hypersensitive peak (e.g., from 440 to 465 nm for Ho(III)) was analyzed.

(39) Legacy waste and spent nuclear fuel rods are dissolved in nitric acid for storage or reprocessing, making nitric acid the best model for liquid−liquid extractions despite strong nitrate ion light absorption below 330 nm.

(40) Rao, L.; Zanonato, P.; Di Bernardo, P.; Bismondo, A. *J. Chem. Soc., Dalton Trans.* **2001**, 1939−1944.

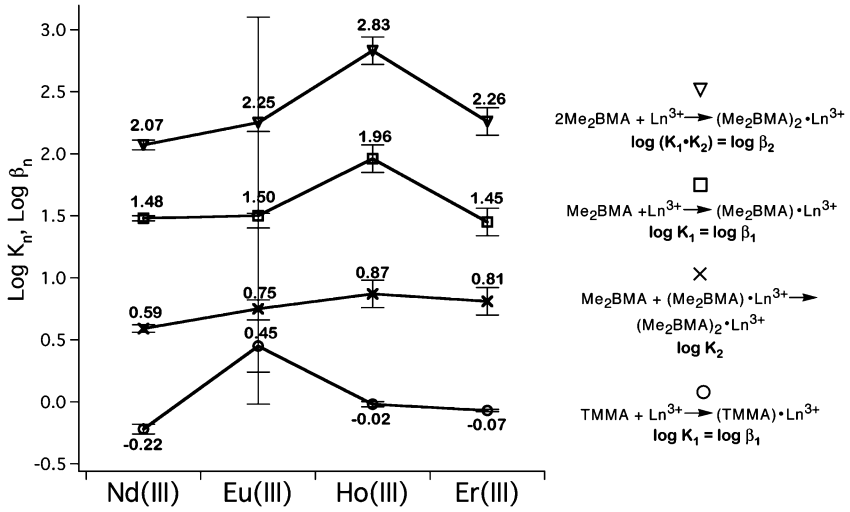


**Figure 2.** Conditional formation constants with error bars determined for bicyclic malonamide $Me_2BMA$ and acyclic malonamide TMMA for the series of trivalent lanthanides. These values were obtained by metal−ligand spectrophotometric titrations in 1 M $HNO_3$ and were refined by SQUAD. The corresponding reactions and formation constants are shown to the right.

The series of spectral segments and their corresponding metal and ligand concentrations were entered into SQUAD.[36]

The conditional binding constants determined from the spectrophotometric titrations are shown in Figure 2. The formation constants refined in the course of this project must be considered conditional because all of the experiments were performed in 1 M $HNO_3$; neither nitrate complexation nor protonation of the ligand was included in the formation constant analysis.[39] However, since both $Me_2BMA$ and TMMA were evaluated under the same conditions, the simplified model does not impact comparison of the resulting values. The overall binding constant for the $ML_1$ complex, log $\beta_1$ (which is equal to the stepwise formation constant, log $K_1$), of $Me_2BMA$ (squares) is 1−2 orders of magnitude greater than that of the $ML_1$ complex formation constant for TMMA (circles).[39] It is expected that the stepwise formation constant for $ML_2$ will be lower because the donated electron density and steric bulk of the first ligand make the $ML_1$ complex a poorer Lewis acid than the free metal ion. $Me_2$-BMA binds strongly enough to form an observable $ML_2$ complex in aqueous 1 M $HNO_3$ (Log $K_2$, Figure 2, ×). Log $K_2$ is not observed for TMMA because it would be less than the already negative values of log $K_1$ and below the limits of log $\beta$ values that can be measured spectrophotometrically (−0.7).[41] The formation of higher ligand−metal ratios is consistent with enhanced binding affinity of the preorganized bicyclic malonamide toward trivalent lanthanides.

There are no apparent trends in binding affinity across the lanthanide series; the values are relatively constant for both the bicyclic and acyclic ligands with the exceptions of higher values for Ho−$Me_2BMA$ and Eu−TMMA. The greater Ho−$Me_2BMA$ affinity is significant because the Ho(III) hypersensitive peak is intense ($\epsilon = 3.90$ cm$^{-1}$ M$^{-1}$), giving a good signal-to-noise ratio and small error. Although the data point for the Eu−TMMA affinity appears to be higher than others in the TMMA−Ln(III) series, the error is large due to the low intensity of the Eu(III) hypersensitive peak ($\epsilon = 0.05$ cm$^{-1}$ M$^{-1}$) and is within experimental error. The low signal-to-noise ratio of the Eu(III) hypersensitive peak also impacts the determination of binding affinity in the Eu−$Me_2BMA$ titration; however, the reported values are similar to the other trivalent lanthanides and within experimental error. The intensity of the LMPHTs at 360−400 and 465 nm present in the spectra for the Eu(III) titration with $Me_2BMA$, though quantitative comparison of the LMPHTs is not possible, supports the overall qualitative observation that $Me_2BMA$ has enhanced binding to Eu(III) over TMMA.

Binding affinities typically follow a trend depending upon the nature of the binding group, making observations from the studies of the BMA ligands difficult to explain without considering preorganization. Bicyclic $Me_2BMA$ has the same binding moiety as acyclic TMMA and should demonstrate similar binding affinities, but fixing the amide carbonyls in a binding conformation results in a significant increase in binding affinity and higher observable ligand−metal ratios across the lanthanide series.

Malonamides are exceptional ligands for lanthanides; it is not usually possible to measure the binding affinity of a neutral ligand in an aqueous solution because of the high enthalpies of hydration for lanthanides, yet these ligands not only successfully compete for binding sites with water but also do so in acidic medium in the presence of excess of nitrate ions. The noted increase in binding affinity of the preorganized ligand supports the original hypothesis that the malonamide ligand extraction efficiency was limited by the energy necessary to rearrange the ligand into the binding conformation. Liquid−liquid extractions are complicated systems with many variables, but the binding affinities reported here are conclusive: preorganizing the ligand binding moiety enhances the binding affinity and contributes to the previously reported $10^7$-fold increase in extraction of Eu(III).[25,30]

**Ligand−Metal Complexes in the Solid State.** The consequences of preorganization of $Me_2BMA$ can be ob-

(41) Hartley, F. R.; Burgess, C.; Alcock, R. M. *Solution Equilibria*; Ellis Horwood Ltd.: Chichester, UK, 1980.

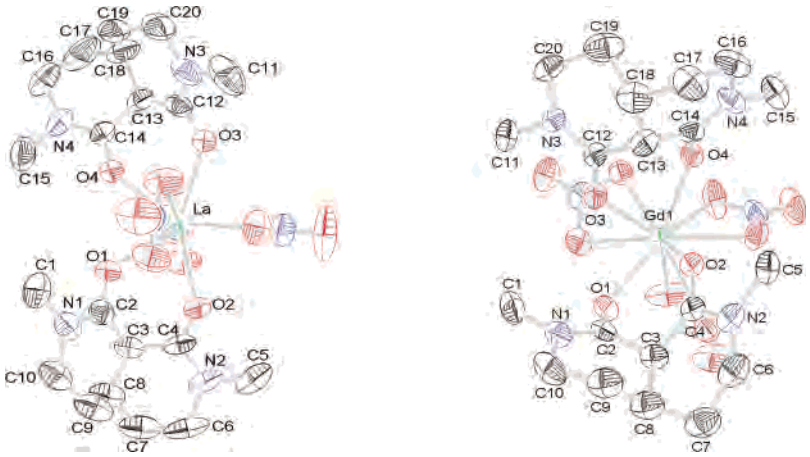


**Figure 3.** ORTEP views demonstrate the two structural arrangements observed in $Me_2BMA$ complexes in this study. The only difference in the structures is the arrangement of the ligands: the La(III) structure (left) has the malonamide ligands separated by a band of nitrate ligands, while the Gd(III) structure (right) exhibits hemispherical grouping of the malonamide and nitrate ligands. Hydrogen atoms have been excluded for clarity. Thermal ellipsoids are shown at 50% probability.

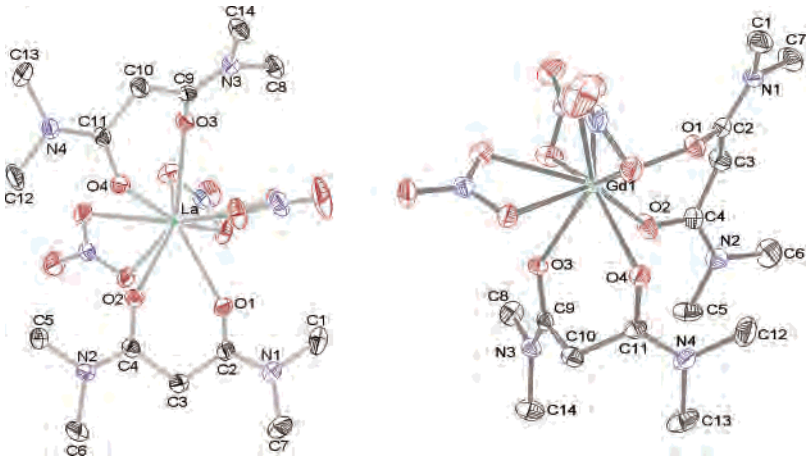


**Figure 4.** ORTEP views demonstrate the two structural arrangements observed in TMMA complexes in this study. The only difference in the structures is the arrangement of the ligands: the La(III) structure (left) has the malonamide ligands separated by a band of nitrate ligands, while the Gd(III) structure (right) exhibits hemispherical grouping of the malonamide and nitrate ligands. Hydrogen atoms excluded for clarity. Thermal ellipsoids are shown at 50% probability.

served in the structural studies, as well as in the measured binding affinities. Comparison of the structures of the bound ligands, $Me_2BMA$ and TMMA, with a series of trivalent lanthanides [La(III), Nd(III), Eu(III), and Gd(III)] was carried out to assess the similarities or differences in ligand organization, structure, or bonding between these malonamides. Comparison of the free $Me_2BMA$ structure to that of the ligand bound to the series of lanthanides directly probes the preorganization of the bicyclic ligand. Finally, comparison of the bicyclic ligand structure predicted by molecular mechanics calculations to the actual crystal structures of the $Me_2BMA$, free and bound, allows qualitative assessment of the success of rational design for the malonamide−lanthanide system.

La(III) and Gd(III) complexes of $Me_2BMA$ and TMMA are shown in Figures 3 and 4 in order to represent all structure types found in this study. Though each structure is unique, it is interesting to note the many similarities. The common feature in all eight structures is the stoichiometry of two malonamides and three nitrates bound to one metal. Both the TMMA− and $Me_2BMA$−La(III) complexes have very similar structures with a band of nitrate ligands separating the malonamides. The malonamides nearly describe a plane which is perpendicular to the band of nitrates ("nitrate-band" structure). The Gd(III) complexes have less in common, but both give the impression of hemispheres because the ligand types group together ("hemispherical" structure). The nitrate ligands are bunched tightly, but the malonamide ligands group differently depending on the type. Stereoviews of these structures are provided in the Supporting Information and may aid the reader in visualizing these structural features.

On the basis of other malonamide−trivalent lanthanide structures,[42] changes in structure correlating to ionic radius are expected. The arrangement of the two different malonamides around the largest metal ion [La(III)] is different from the arrangement around the smallest metal ion [Gd(III)]. The different arrangement may be due to formation of more-stable ligand shells with decreasing ionic radius. Perhaps of more interest is that the small-ion [Gd(III)] complex represents a

(42) Den Auwer, C.; Charbonnel, M. C.; Drew, M. G. B.; Grigoriev, M.; Hudson, M. J.; Iveson, P. B.; Madic, C.; Nierlich, M.; Presson, M. T.; Revel, R.; Russell, M. L.; Thuery, P. *Inorg. Chem.* **2000**, *39*, 1487−1495.

**Table 2.** Averaged Bond Lengths and Angles of the Free Bicyclic Ligand Compared to Lanthanide Complexes with Bicyclic and Acyclic Ligands[a]

| | free ligand | $La L_2 (NO_3)_3$ | | $Nd L_2 (NO_3)_3$ | | $Eu L_2 (NO_3)_3$ | | $Gd L_2 (NO_3)_3$ | |
|---|---|---|---|---|---|---|---|---|---|
| | $Me_2$BMA | $Me_2$BMA | TMMA | $Me_2$BMA | TMMA | $Me_2$BMA | TMMA | $Me_2$BMA | TMMA |
| | | | | Length (Å) | | | | | |
| M−O | − | 2.499 (13) | 2.502 (26) | 2.443 (17) | 2.447 (27) | 2.395 (16) | 2.404 (34) | 2.384 (15) | 2.385 (17) |
| O−C | 1.222 (3) | 1.243 (7) | 1.257 (10) | 1.25 (2) | 1.251 (8) | 1.243 (19) | 1.26 (0) | 1.245 (15) | 1.251 (4) |
| C−C* | 1.528 (5) | 1.518 (20) | 1.511 (15) | 1.52 (1) | 1.511 (6) | 1.519 (17) | 1.50 (2) | 1.525 (4) | 1.510 (12) |
| C−N | 1.351 (0) | 1.321 (9) | 1.331 (11) | 1.32 (1) | 1.329 (2) | 1.322 (13) | 1.32 (1) | 1.325 (5) | 1.328 (9) |
| | | | | Angle (deg) | | | | | |
| O−M−O | − | 69.0 (3) | 66.1 (4) | 69.6 (10) | 67.2 (4) | 70.5 (11) | 68.0 (4) | 70.9 (10) | 71.7 (26) |
| M−O−C | − | 133.6 (68) | 133.0 (61) | 132.6 (54) | 133.3 (68) | 132.7 (50) | 133.1 (73) | 132.4 (47) | 132.5 (45) |
| O−C−C* | 121.0 (1) | 120.0 (16) | 120.6 (12) | 119.8 (13) | 120.7 (10) | 119.4 (20) | 119.7 (20) | 119.4 (13) | 119.9 (22) |
| O−C−N | 122.0 (4) | 121.0 (20) | 120.6 (11) | 121.0 (10) | 120.8 (10) | 121.3 (19) | 120.8 (11) | 121.5 (7) | 120.8 (6) |
| C−C*−C | 109.9 (−) | 109.4 (7) | 113.2 (0) | 109.8 (7) | 113.1 (3) | 108.9 (7) | 114.0 (8) | 108.7 (4) | 111.0 (38) |
| N−C−C* | 117.1 (3) | 119.0 (13) | 118.8 (13) | 119.2 (10) | 118.5 (14) | 119.2 (10) | 119.4 (12) | 119.1 (6) | 119.3 (20) |

[a] Selected bond lengths (Å) and bond angles (deg) from crystal structures of bicyclic malonamide $Me_2$BMA and acyclic malonamide TMMA with a series of lanthanide nitrate salts. This table assumes that the oxygens, nitrogens and carbons of the chelate ring are self-similar, with the exception of the bridgehead carbon, C2 = C*. These values are thus the *average* of the similar bonds or angles in any one crystal structure and represent two or four values each. The value in parentheses represents the range of the final digits [e.g., "120.6 (11)" is an average of 120.6 from values which range from 119.5 to 121.7, while "1.251 (4)" is an average of 1.251 from values which range from 1.247 to 1.255.] The complete table with actual values and errors is included in the Supporting Information.

**Table 3.** Selected Dihedral Angles and Carbonyl Plane Angle from Crystal Structures of Bicyclic Malonamide $Me_2$BMA and Acyclic Malonamide TMMA with a Series of Lanthanide Nitrate Salts[a]

| | free ligand | $La L_2 (NO_3)_3$ | | $Nd L_2 (NO_3)_3$ | | $Eu L_2 (NO_3)_3$ | | $Gd L_2 (NO_3)_3$ | |
|---|---|---|---|---|---|---|---|---|---|
| | $Me_2$BMA | $Me_2$BMA | | $Me_2$BMA | | $Me_2$BMA | | $Me_2$BMA | |
| M−O1−C1−C2 | − | −59.6(5) | −63.4(5) | −36(1) | −55(1) | −38.6(7) | −57.0(7) | −37.9(6) | −56.4(5) |
| M−O2−C3−C2 | − | −16.2(7) | −15.6(7) | −32(1) | −20(1) | −31.5(7) | −17.0(8) | −31.9(5) | −19.2(6) |
| M−O1−C1−N1 | − | 122.5(4) | 120.1(4) | 144.3(7) | 127.4(8) | 144.6(4) | 126.0(5) | 145.6(3) | 125.4(4) |
| M−O2−C3−N2 | − | 162.1(3) | 160.8(3) | 145.2(7) | 157.7(7) | 146.7(4) | 159.3(4) | 145.9(3) | 157.7(3) |
| O1−C1−C2−C3 | 28.2(2) | 73.2(5) | 67.4(5) | 63(1) | 73(1) | −33.7(6) | −29.2(7) | 64.5(5) | 71.5(5) |
| C1−C2−C3−O2 | −82.9(2) | −33.0(6) | −27.1(6) | −28(1) | −34(1) | 72.2(6) | 64.2(7) | −29.2(5) | −32.3(5) |
| carbonyl planes | 54.7(2) | 40.2(6) | 40.3(6) | 35(1) | 39(1) | 38.5(6) | 35.0(7) | 35.3(5) | 39.2(5) |
| | | TMMA | | TMMA | | TMMA | | TMMA | |
| M−O1−C1−C2 | − | 51.6(4) | −69.0(3) | 48.0(3) | −68.2(2) | −68.8(9) | 58(1) | −45.8(4) | 35.9(3) |
| M−O2−C3−C2 | − | 58.4(4) | −57.6(4) | 155.3(2) | −55.6(3) | −56(1) | 47(1) | −27.2(4) | −55.2(3) |
| M−O1−C1−N1 | − | −131.6(3) | 114.6(3) | −135.4(2) | 115.1(2) | 115.9(7) | −1265(8) | 134.3(2) | −142.8(2) |
| M−O2−C3−N2 | − | −123.2(3) | 125.2(3) | −125.9(2) | 127.1(2) | 128.6(7) | −138.3(8) | 156.9(2) | 122.6(2) |
| O1−C1−C2−C3 | − | −30.6(4) | 25.7(4) | −27.9(3) | 23.9(3) | 24(1) | −20(1) | −9.2(4) | −59.0(3) |
| C1−C2−C3−O2 | − | −19.0(4) | 34.3(4) | −18.7(3) | 34.9(3) | 35(1) | −27(1) | 44.1(4) | 71.3(3) |
| carbonyl planes | | 49.6(4) | 60.0(4) | 46.6(3) | 58.8(3) | 59(1) | 47(1) | 34.9(4) | 12.3(3) |

[a] Figure A is an explanation of how the angle between the carbonyl planes was determined. The dihedral angle of the atoms A−B−C−D is determined as the angle between A and D when viewed down the B−C bond (clockwise is positive, counterclockwise is negative). The dihedral angles O1−C1−C2−C3 ($\theta_1$) and C1−C2−C3−O2 ($\theta_2$) can be added together to determine the angle between the carbonyl planes ($\theta_3$) because (1) the three shared atoms (C1−C2−C3) describe a plane from which the carbonyl oxygens depart and (2) the carbonyls are fixed in the same relative direction by the O−M bonds. The generic numbering scheme used in Tables 2 and 3 for the chelate ring (A) and specific numbering schemes (B) for both ligands as found in the CIF files are shown on the following structures. The bridgehead hydrogens on the bicyclic structures are pointing into the page.

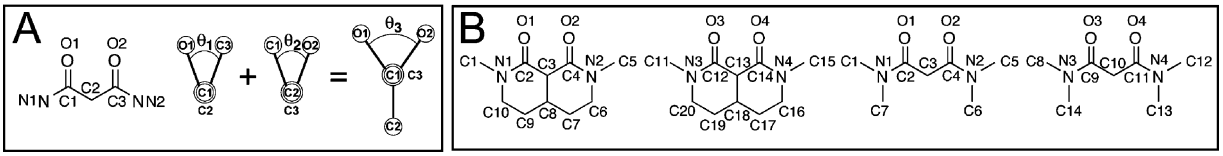


structure distinct within the TMMA series, while the large-ion [La(III)] complex has a structure distinct from the series with $Me_2$BMA. TMMA complexes form the nitrate-band structure for La(III), Nd(III), and Eu(III), switching to the hemispherical structure for Gd(III). Interestingly, La−$Me_2$-BMA is the only complex in this ligand series which forms the nitrate-band structure; the Nd(III), Eu(III), and Gd(III) complexes all form the hemispherical structure.

Refinement and analysis of the crystal structures allows quantitative comparison of the ligand bond lengths and angles between free $Me_2$BMA and lanthanide-bound $Me_2$BMA, as well as between lanthanide-bound $Me_2$BMA and TMMA. Table 2 shows selected bond lengths and angles pertaining to the atoms that form the chelate ring when the ligand binds a lanthanide ion. For ease of comparison of bond lengths and angles in Table 2, the atoms of interest have been labeled the same. The key to the structure labeling can be found in the caption of Table 3, with a generic numbering scheme used in Table 2 and the other structures showing the actual numbering scheme applied to the ligands in the Supporting Information (tables and crystallographic information files).

Close examination of the bond lengths, bond angles, and dihedral angles (see Table 3) for both $Me_2$BMA and TMMA complexes shows little difference between the resulting chelate rings formed by the two ligand types despite the various structure types. All of the complexes reported here are ten coordinate, but the metal−oxygen (of the amides) bond lengths are shorter than those predicted from the ionic

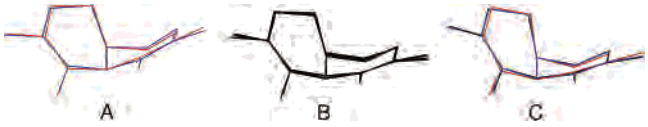


**Figure 5.** Superposition of various structures of the bicyclic malonamide $Me_2BMA$ reveal their similarity. A is an overlay of the computed (blue) and experimental (red) forms of the free ligand. B is an overlay of experimental (black) forms of bound ligands taken from crystal structures of the Nd(III), Eu(III), and Gd(III) complexes. C is the same as A but includes a representative bound ligand (black) from the crystal structure of the Gd(III) complex.

radii of nine-coordinate trivalent lanthanides.[43] (Increased coordination number should result in longer M−O bond lengths, not shorter.) In these structures, the C−O bond lengths do not change for either $Me_2BMA$ or TMMA, indicating that the ligands bind equally well to trivalent lanthanides across the series. These strong similarities between $Me_2BMA$ and TMMA in the final complexes is unsurprising and indeed, anticipated, because the binding moiety is chemically identical. The similarities found within the complexes indicate that preorganization does not change the nature of the resulting metal−ligand bond, indicating once again that the improvements in binding affinity are a result of the reduced steric cost of complex formation.

The final parameter listed in Table 3 is the angle between the carbonyl planes, which provides another indicator of the degree of preorganization of the ligand. The values for Ln(III)−$Me_2BMA$ complexes are compared to the values for Ln(III)−TMMA complexes and for $Me_2BMA$ measured as the free ligand. There are no experimental data to confirm the initial carbonyl orientations in TMMA. However, conformational analysis of TMMA at the MP2/aug-cc-pVTZ level of theory establishes the most stable "gas-phase" conformer occurs when the carbonyl groups are pointed in opposite directions (180°) in order to balance the dipole.[26] To form the TMMA complex, the ligand must rearrange to reduce the angle between the carbonyl planes to 12−60°, an overall rotation of 120−170°. In contrast, unbound $Me_2BMA$ measures 54.7° between the carbonyl planes. Upon binding, the ligand rearranges to decrease this angle to 35−40°, a change of only 15−20°. Thus, although TMMA is able to approach the ideal conformation, there is significant structural reorganization that is required to achieve it. Although $Me_2BMA$ is not perfectly arranged, smaller changes to the structure are needed for binding to occur.

The small magnitude of the conformational changes that occur within the $Me_2BMA$ ligand upon binding trivalent lanthanides are emphasized by overlaying wire frames of the ligands. An overlay of the predicted (blue) and experimental (red) structures for uncomplexed $Me_2BMA$, Figure 5A, shows that the molecular mechanics calculations give a good estimate of the X-ray structure for the free ligand. Figure 5B shows that $Me_2BMA$ is in the same conformation when bound (black) across the series of trivalent lanthanides Nd(III), Eu(III), and Gd(III). The small degree of change from the conformation of the free ligand (blue and red) to the conformation of the ligand bound to a representative trivalent lanthanide ion (black), Figure 5C, combined with the significant increase in binding affinity over the acyclic ligand, demonstrates that the bicyclic ligand is preorganized.

Crystallographic analysis of the trivalent lanthanide complexes of $Me_2BMA$ confirms preorganization of the binding site. Bond lengths and angles of $Me_2BMA$ are nearly identical to those of TMMA when bound to the same metal ions, which was expected because the binding moiety was not changed. The only observable difference between the binding of the bicyclic and acyclic ligands is their preferred stacked or perpendicular orientations when bound to the metal ion.

## Conclusions

Rational ligand design is a viable, useful tool for the discovery of high-affinity ligands for new uses and applications. Assessment of ligand−metal interactions and determination of a substructure that fixes the ligand into the desired binding conformation has led to preorganized ligands that exhibit enhanced binding affinity over the original ligand. Through solution experiments with a series of trivalent lanthanides, we have demonstrated that $Me_2BMA$ has an enhanced binding affinity when compared to acyclic TMMA. The increased binding affinity directly and conclusively confirms the enhanced performance that was predicted and initially demonstrated by increased extraction efficiency of Eu(III). Through crystallographic studies with a similar series of trivalent lanthanides, we have demonstrated that the enhanced binding affinity is a direct result of the preorganization of the binding site. The binding moieties of $Me_2BMA$ and TMMA are identical and bind in the same manner, as is shown in the crystal structures; thus, the only reasonable explanation for the enhancement in the binding affinity is the only difference in the ligands: preorganization of the binding site. Preorganization of the malonamide ligand system has been demonstrated in the increased binding affinity and increased ability for multiple bicyclic malonamide ligands to bind competitively in the presence of excess protons, water, and nitrate ions. These noted enhancements are significant contributors to the $10^7$-fold enhancement of the extraction efficiency we previously reported.[25]

**Acknowledgment.** We thank Dr. Scott T. Griffin (The University of Alabama) for his assistance in preparing the CIF files of several of the Ln−TMMA compounds. B.W.P., R.D.G, J.E.H., E.R.H., and T.J.R.W. acknowledge support from the National Science Foundation (CHE-0213563) and the NSF IGERT (DGE−0114419). B.M.R., B.P.H., and S.I.S. acknowledge support from the Environmental Management Science Program, Office of Science, U.S. Department of Energy (Grant 73759). R.D.R would like to acknowledge funding at The University of Alabama by the Division of Chemical Sciences, Geosciences, and Bioscience, Office of Basic Energy Research, U.S. Department of Energy (DE-FG02-96ER14673). The research was performed at the University of Oregon, the Pacific Northwest National Laboratory [operated by Battelle for the Department of Energy (DE-AC06-76RL01830)], and The University of Alabama.

(43) Shannon, R. D. *Acta Crystallogr.* **1976**, *32*, 751−767.

**Supporting Information Available:** Table of conditional binding constants with errors corresponding to Figure 2; stereoviews of the complexes La−TMMA, La−$Me_2$BMA, Gd−TMMA, and Gd−$Me_2$BMA; expanded table of selected bond lengths, bond angles, and dihedral angles with errors corresponding to Tables 2 and 3; and complete tables and CIF files for $Me_2$BMA and complexes of TMMA and $Me_2$BMA with La(III), Nd(III), Eu(III), and Gd(III). This material is available free of charge via the Internet at http://pubs.acs.org.

IC050437D